Heliyon 10 (2024) e24988

Contents lists available at ScienceDirect

Heliyon

journal homepage: www.cell.com/heliyon

Research article

Erzhi pills reverse PD-L1-mediated immunosuppression in melanoma microenvironment

Zhirui Fang [a,b,1], Yuejin Xue [a,b,1], Yuze Leng [b,1], Lusha Zhang [a,b], Xiuyun Ren [a,b], Ning Yang [d], Jing Chen [d,**], Lu Chen [a,c,*], Hong Wang [a,b,***]

[a] State Key Laboratory of Component-based Chinese Medicine, Tianjin University of Traditional Chinese Medicine, 301617, Tianjin, China
[b] School of Medical Technology, Tianjin University of Traditional Chinese Medicine, 301617, Tianjin, China
[c] Instrumental Analysis and Research Center, Tianjin University of Traditional Chinese Medicine, 301617, Tianjin, China
[d] Second Affiliated Hospital of Tianjin University of Traditional Chinese Medicine, Department of Dermatology, 300250, Tianjin, China

ARTICLE INFO

Keywords:
EZP
Melanoma
PD-L1
T cells
Cancer immunotherapies

ABSTRACT

Background: Cancer immunotherapies aimed at activating immune system, especially by blocking immune checkpoints, have become a successful modality for treating patients with advanced cancers. However, its clinical practice is frequently conceded by high outcomes, low initial response rates and severe side effects. New strategies are necessary to complement and advance this biological therapy. Erzhi Pills (EZP) have diverse pharmaceutical effects including immune regulation, anti-tumor and anti-senescence. We hypothesized that EZP could exert its antitumor effect through immunomodulation.

Purpose: The aim of this study was to investigate the effects of EZP on anti-tumor activities, and define its molecular mechanisms.

Methods: By applying melanoma model with high immune infiltrates, we determined the anti-melanoma effect of EZP. To identify whether this effect was mediated by direct targeting tumor cells, cell viability and apoptosis were examined *in vitro*. Network pharmacology analysis was used to predict the potential mechanisms of EZP for melanoma via immune response. Flow cytometry, immunohistochemistry (IHC), enzyme-linked immunosorbent assay (ELISA) and crystal violet (CV) experiments were performed to detect T cell infiltrations and functions

Abbreviations: EZP, Erzhi Pill; TCM, traditional Chinese medicines; DTIC, Dacarbazine; CTLA-4, cytotoxic T lymphocyte-associated molecule-4; PD-1, programmed cell death receptor-1; PD-L1, programmed cell death ligand-1; IFN-γ, interferon-γ; MTT, 3-(4,5-dimethylthiazol-2-yl)-2,5-diphenyltetrazolium bromide; DMSO, dimethylsulfoxide; PBS, phosphate-buffered saline; PFA, paraformaldehyde; EDTA, ethylene diamine tetra-acetic acid; RBC, red blood cell; BSA, bovine serum albumin; IHC, immunohistochemistry; P/S, penicillin/streptomycin; HI-FBS, heat-inactivated fetal bovine serum; TBS-T, Tris-buffered saline-Tween-20; GZMB, granzyme B; LLF, *Ligustri lucidi fructus*; EH, *Ecliptae herba*; Bcl-2, B-cell lymphoma-2; Bax, Bcl-2 associated X protein; Bcl-xl, Bcl-2 like 1; STAT, signal transducer and activator of transcription; p-STAT1, phospho-STAT1; NF-κB, nuclear factor kappa-B; RELA, NF-κB p65; GAPDH, glyceraldehyde 3-phosphate dehydrogenase; CV, crystal violet; LDH, lactate dehydrogenase; ELISA, enzyme-linked immunosorbent assay; IL-2, interleukin-2; CAR, chimeric antigen receptor; NK, natural killer.

* Corresponding author. State Key Laboratory of Component-based Chinese Medicine, Tianjin University of Traditional Chinese Medicine, 301617, Tianjin, China.

** Corresponding author. Second Affiliated Hospital of Tianjin University of Traditional Chinese Medicine, Department of Dermatology, 300250, Tianjin, China.

*** Corresponding author. School of Medical Technology, Tianjin University of Traditional Chinese Medicine, 301617, Tianjin, China.

E-mail addresses: chenjing@tjzyefy.com (J. Chen), chenlutjutcm@tjutcm.edu.cn (L. Chen), wanghongsys@tjutcm.edu.cn (H. Wang).

[1] These authors have contributed equally to this work.

https://doi.org/10.1016/j.heliyon.2024.e24988
Received 23 November 2023; Received in revised form 17 January 2024; Accepted 17 January 2024
Available online 18 January 2024

mediated by EZP. The mechanism of EZP was further investigated by western blotting both *in vivo* and *in vitro*.
Results: The administration of EZP significantly inhibited tumor weight and volume. EZP extract could only slightly reduce cell viability and induce melanoma apoptosis. Network pharmacology analysis predicted that JAK-STAT signaling pathway and T cell receptor signaling pathway might be involved during EZP treatment. Flow cytometry and IHC analyses showed that EZP increased the number of $CD4^+$ T cells and enhanced the function of $CD8^+$ T cells. In co-culture experiments, EZP elevated killing ability of T cells. Western blotting showed that EZP treatment reduced PD-L1 signaling pathway.
Conclusion: These findings indicated that EZP exerted anti-melanoma effects by inducing apoptosis and blocking PD-L1 to activate T cells. EZP might represent a promising candidate drug for cancer immunotherapies.

1. Introduction

Cancer cells can evade from immune surveillance by binding immune checkpoint-specific ligands to prevent immunogenic cell death [1,2]. During the last decade, cancer immunotherapies aimed at activating immune system to recognize and eliminate tumor cells, especially by blocking immune checkpoints, have become a successful modality for treating patients with advanced cancers [3,4]. Programmed cell death receptor 1 (PD-1) and programmed cell death ligand 1 (PD-L1) checkpoint inhibitors are widely applied in clinic to attack malignant cells. Meanwhile, the clinical practice of immunotherapy is frequently conceded by high outcomes, low initial response rates and severe side effects [5,6]. New strategies are necessary to complement and advance this biological therapy.

Traditional medicines are gaining increasing popularity in cancer treatment due to low toxic effects, lack of drug resistance, and convenient administration [7–9]. Erzhi pills (EZP) are composed of *Ligustri lucidi fructus* (LLF, *Ligustrum lucidum Ait.*) and *Ecliptae herba* (EH, Eclipta *prostrat*a L.) on the ratio of 1: 1 and have diverse pharmaceutical effects including immune regulation and anti-senescence [10,11]. In the clinical practices, EZP was used to prevent and treat breast cancer [12]. Network pharmacology predicted that EZP could inhibit skin cutaneous melanoma. Given the immunoregulatory, anti-aging and antineoplastic effects reported for EZP, we hypothesized that EZP could exert its antitumor effect through immunomodulation. The aim of this study is to define molecular mechanisms of EZP using melanoma model to supply pharmacological proof supporting its clinical employment.

2. Methods

2.1. Chemicals and reagents

EZP (Z36021716) was obtained from Jiangxi Yaodu Zhangshu Pharmaceutical Co., Ltd (Jiangxi, China). Dacarbazine (DTIC, HY-B0078) and polyethylene glycol 300 (PEG300, HY-Y0873) were purchased from MedChemExpress (NJ, USA). Dimethylsulfoxide (DMSO, 20–139), 3-(4,5-dimethylthiazol-2-yl)-2,5-diphenyltetrazolium bromide (MTT, M2128), tribromoethanol (T48402) and *tert*-amylalcohol (152463) were obtained from Sigma-Aldrich (MO, USA). Recombinant murine interferon-γ (IFN-γ, 315-05) was purchased from PeproTech (NJ, USA). Phosphate-buffered saline (PBS, P1020), 4 % paraformaldehyde (PFA, P1110), ethylene diamine tetraacetic acid (EDTA, E8040) and red blood cell (RBC, R1010) lysis buffer were provided from Solarbio (Beijing, China). 0.9 % sterile saline (1501251) was purchased from Guangdong Otsuka Pharmaceutical Co., Ltd (Guangdong, China). Bovine serum albumin (BSA, 4240GR100) was purchased from Biofroxx (Einhausen, Germany). Tween-20 (T6335) was provided from Macklin (Shanghai, China). Immunohistochemistry (IHC) kit (SA1022) was purchased from Boster (Wuhan, China).

2.2. Extract preparation

EZP extract was prepared by the Tianjin State Key Laboratory of Modern Chinese Medicine of Tianjin university of Traditional Chinese Medicine.

2.3. Animals

A total of 40 clean specific pathogen-free grade female C57BL/6 mice (weight, 20–25 g; age, 6–8 weeks) were purchased from Beijing Weitong Lihua Experimental Animal Technology Co., Ltd. (Beijing, China). The protocols for *in vivo* study were approved by the Ethics Committee of Tianjin University of Traditional Chinese Medicine (approval number TCM-LAEC2021214, registered on February 10, 2021). Animal rooms were maintained a standard rearing environment at a temperature of 23 ± 2 °C, 50 ± 10 % humidity and a 12-h light/dark cycle. Free food and water intake and adaptive feeding was allowed for a week prior to initiation.

2.4. Cell culture and drug treatment

Jurkat cells (BNCC338675) were purchased from Beina Bio (Beijing, China). A375 human melanoma cells and B16F10 mouse melanoma cells were derived from our laboratory depository. A375 and B16F10 cells were cultured in DMEM with high glucose

containing 1 % penicillin/streptomycin (P/S) and 10 % heat-inactivated fetal bovine serum (HI-FBS) at 37 °C in 5 % CO_2 incubator. Jurkat cells were maintained in RPMI 1640 containing 10 % HI-FBS and 1 % P/S. Cell culture reagents were purchased from Biological Industries (BI, Kibbutz, Israel) unless otherwise mentioned. Some western blotting experiments, A375 and B16F10 cells adjusted the cell density to 1.5×10^5 cells/mL were seeded into 6-well plates and treated with 0.1 % DMSO and 1 μg/mL EZP extract for 48 h. To induce the maximum expression of PD-L1, A375 cells (1×10^5 cells/mL) were cultures into 96-well plates and treated with 10 ng/mL IFN-γ for 24 h in culture media. Afterwards, A375 cells were administrated with 0.1 % DMSO, different EZP extract concentrations (0.01, 0.1, 1 μg/mL) for 48 h.

2.5. Melanoma model and treatment

Animals were randomly divided into five groups of eight animals each: one control group and four treatment groups. B16F10 mouse melanoma cells (6×10^4 cells) in 200 μL PBS were injected subcutaneously into the right flank of C57BL/6 female mice. Following tumor inoculation, the control group was treated with 0.9 % sterile saline whereas the other groups received DTIC and varying doses of EZP. EZP was dissolved in 0.9 % sterile saline and administered by gavage at 0.59, 1.17 and 2.34 g/kg/day for 14 consecutive days. As a positive control, DTIC (70 mg/kg) was suspended in a 50:50 mix of 0.9 % sterile saline and PEG300 and provided to mice by intraperitoneal injection every 2 days on fourth day after inoculation. Treatments were started immediately after the injection of the B16F10 cells and continued until day 14, when mice were sacrificed. Tumor length (L) and width (W) were measured using a calliper, and the tumor volume was calculated as $L \times W^2 \times 0.5$.

At the end of the experiment, tumor tissues were collected, weighed, frozen in liquid nitrogen and stored at −80 °C until use or 4 % PFA fixed and paraffin embedded for subsequent sectioning. Meanwhile, single cell suspensions of spleen were prepared.

2.6. MTT assays

Cell viability was detected using MTT assays. In brief, A375 and B16F10 cells in logarithmic growth phase were seeded in 96-well plates and treated with DMSO or different EZP extract concentrations (0.001, 0.01, 0.1, 1 μg/mL) for 24, 48 and 72 h. The supernatant was discarded and then 20 μL MTT reagent (5 mg/ml) was added to each well and incubated for 4 h and then terminated by adding 150 μL DMSO and incubating at 37 °C in the dark for 15 min. OD value was assessed by measuring the absorbance at 570 nm (Molecular Device Flex Station® 3, Silicon Valley, USA).

2.7. Western blotting

Shortly, 20 μg proteins from tumors or cultured cells were separated on sodium dodecyl sulfate-polyacrylamide gel electrophoresis and then electrotransferred onto polyvinylidene fluoride membranes. Next, membranes were blocked in Tris-buffered saline-Tween-20 (TBS-T) (5 % non-fat powdered milk, 0.2 % Tween 20) and washed thrice with TBS-T (2 % Tween 20). The membranes were incubated with the primary antibodies against PD-L1 (A18103, Abclonal, Wuhan, China), caspase-3 (#14220), cleaved-caspase-3 (#9664), B-cell lymphoma-2 (Bcl-2, #3498), Bcl-2 like 1 (Bcl-xl), Bcl-2 associated X protein (Bax, #2772), signal transducer and activator of transcription (STAT) 1 (#14994), phospho-STAT1 (p-STAT1, #9167), nuclear factor kappa-B (NF-κB) p65 (RELA, #8242) and glyceraldehyde 3-phosphate dehydrogenase (GAPDH) (#5174, Cell Signaling Technology, CST, MA, USA) in 5 % BSA in TBS-T overnight at 4 °C and followed by exposure to the secondary horseradish peroxidase-labeled goat anti-rabbit IgG (H + L) (ZB-2301, Beijing ZSGB-BIO Technology Co., Ltd., Beijing, China) for 1 h at room temperature. Then the blots were developed by Super ECL Detection Reagent (36208ES60, YEASEN, Shanghai, China). The protein bands were photographed using a gel imaging system (Amersham Imager 680, GE, Boston, USA). Finally, results were analyzed by image J software (Image J, NIH).

2.8. Network pharmacology

The drug-likeness and the physicochemical properties of the selected hits of EZP were evaluated using PubChem database (https://pubchem.ncbi.nlm.nih.gov/), SwissADME database (www.swissadme.ch) and TCMSP database (http://tcmspw.com/tcmsp.php). Related targets of EZP were selected using TCMSP database and SwissTargetPrediction database (http://www.swisstargetprediction.ch/). Targets of melanoma and immune response were collected using GeneCards database (https://www.genecards.org/) and comparative toxicogenomics database (CTD, http://ctdbase.org/). We intersected the obtained drug targets with the targets associated with melanoma and immune response, and obtained a Venn diagram of the common targets. Based on the results of protein-protein interaction (PPI) in STRING database (https://string-db.org), the Cytoscape 3.7.2 software was used to construct the PPI network. Based on the PPI network, the plug-in "CytoHubba" was used to calculate the degree values of nodes in the network. Gene ontology (GO) functional enrichment analysis and kyoto encyclopedia of genes and genomes (KEGG) pathway enrichment analysis were performed using the DAVID database (https://david.ncifcrf.gov/).

2.9. Flow cytometry

Splenocytes were isolated by mechanical disruption from the freshly obtained spleen of each group mice and passed through a 70 μm cell strainer to prepare cell suspensions. After removal of RBC using RBC lysis buffer, cell suspensions were surface labeled with mouse antibodies for 30 min at 4 °C. After staining, the cells were washed once with PBS and resuspended in staining buffer (PBS, 2 mM

EDTA, 2 % HI-FBS). Finally, samples were assessed using BD Accuri™ C6 plus (BD Biosciences, CA, USA) and analyses were performed using FlowJo. PerCP/Cyanine5.5 anti-mouse CD3 antibody (E-AB-F1013J), FITC anti-mouse CD8a antibody (E-AB-F1104C) and PE anti-mouse CD4 antibody (E-AB-F1097D) were obtained from Elabscience (Wuhan, China).

2.10. Immunohistochemistry

IHC stainings of CD4, CD8 and granzyme B (GZMB) were performed on paraffin-embedded tumor sections. After deparaffinization, rehydration, antigen retrieval, endogenous peroxidase inactivation and blocking non-specific binding, the 5 μm-thick sections were incubated with primary anti-CD4, anti-CD8 and GZMB antibodies overnight at 4 °C. Then, the slides were incubated with a corresponding secondary antibody and photomicrographs were taken utilizing a Nikon Eclipse E400 microscope (Nikon, Tokyo, Japan). Quantitative IHC data for CD4, CD8 and GZMB marker was calculated by counting the number of $CD4^+$, $CD8^+$ and $GZMB^+$ cells in three fields at 400 × magnification. CD4 (D7D2Z, #25229), CD8 (D4W2Z, #98941) and GZMB (E5V2L, #44153) antibodies were purchased in CST.

2.11. Co-culture of Jurkat and A375 cells

We constructed an *in vitro* co-culture model to model the tumor microenvironment. Briefly, cultures containing either Jurkat, A375 cells or both were established in 12-well plates containing DMEM with 10 % FBS and 1 % P/S. As target cells, A375 cells were seeded in 96-well plates at a density of 5×10^5/well and treated with 0.1 % DMSO and different EZP extract doses (0.01, 0.1, 1 μg/mL) for 4 h. Next, A375 cells were stimulated with IFN-γ (10 ng/mL) for 24 h. Jurkat cells, acting as effector cells, were stimulated by simultaneously activating the T-cell receptor/CD3 complex and CD28 coreceptor with purified anti-human CD3 antibody (317301) and purified anti-human CD28 antibody (302901, BioLegend, CA, USA). For co-cultures, Jurkat cells were added to the target cells at an effector-to-target (E:T) ratio of 10:1 and were allowed to attach for 72 h at 37 °C in 5 % CO_2 incubator.

2.12. Crystal violet staining

After 72 h of culture, the co-cultured cells were harvested for further analysis. For the crystal violet (CV) staining, cells were fixed with 4 % PFA and stained with 0.1 % CV (C0121, Beyotime, Shanghai, China) for 10 min and washed with distilled H_2O to removed excessive staining solution. Finally, Images were captured by a Nikon Eclipse Ts2 microscope (Nikon, Tokyo, Japan) and counted by ImageJ.

2.13. Lactate dehydrogenase assay

Culture supernatants were collected after 72 h of co-culture. Lactate dehydrogenase (LDH) was measured by the LDH assay kit (A020-1, Nanjing Jiancheng Bioengineering Institute, Nanjing, China) according to the manufacturer's instructions. The absorbance

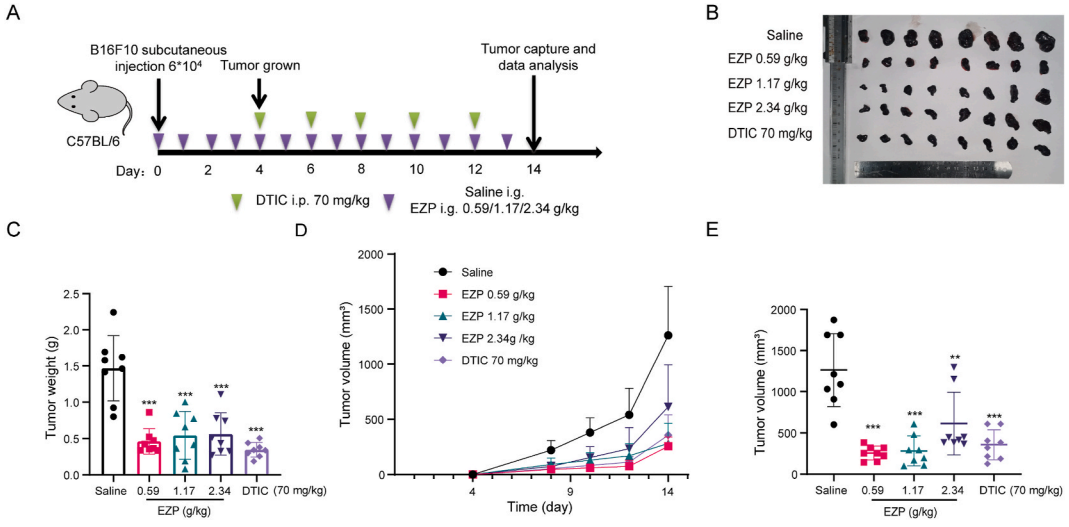

Fig. 1. EZP provided therapeutic benefit in B16F10 tumor-bearing mice. (A) A schematic view of the treatment plan. C57BL/6 mice were implanted with B16F10 mouse melanoma cells (6×10^4 cells) in 200 μL PBS and received EZP (0.59, 1.17, 2.34 g/kg) treatment or DTIC (70 mg/kg). (B) Photograph of tumor tissues. (C) Summary of weight data of B16F10 tumors harvested after euthanizing the mice. (D) Plots of tumor volumes and mice body weight measured every 2 days. (E) Summary of volume data of B16F10 tumors harvested after euthanizing the mice. Data are expressed as mean ± SD. n = 8. $^{**}P < 0.01$ and $^{***}P < 0.001$ vs saline. EZP, erzhi pill; DTIC, dacarbazine.

value of each well was measured with Molecular Device Flex Station® 3 at 450 nm. The harvested media were used for immunoblotting and enzyme immunoassay.

2.14. Enzyme-linked immunosorbent assay

The co-culture supernatants were collected for enzyme-linked immunosorbent assay (ELISA). Interleukin-2 (IL-2) was performed using the human IL-2 ELISA kit (JYM0146Hu, Wuhan jiyinmei Biotechnology Co., Ltd., Wuhan, China) according to manufacturer's guidelines.

2.15. Statistical analysis

All data are presented as means ± standard deviation (SD). The differences between the two groups were analyzed by performing unpaired Student's *t*-tests. GraphPad prism 8.0 was used for the statistical analysis. *P* value of less than 0.05 was considered statistically significant.

3. Results

3.1. EZP administration inhibited melanoma growth

Considering EZP possessed pharmacological effects of tonics, immune regulation and anti-tumor activity , we testified the preventive efficacy of EZP on tumor growth *in vivo* using melanoma-bearing C57BL/6 mice (Fig. 1A). The administration of EZP (0.59, 1.17, 2.34 g/kg) significantly inhibited tumor weight and volume (Fig. 1B–E), indicating EZP provided potential benefit in retarding melanoma development.

To identify whether this anti-melanoma effect was mediated by direct targeting tumor cells, two melanoma cell lines (B16F10 and A375) were applied to examine the viability of melanoma cells under the treatment of EZP. As shown in Fig. 2A and B, EZP extract could only slightly reduce cell viability. We further detected the expressions of apoptosis-related proteins after treatment with 1 μg/mL EZP extract for 48 h based on the results of cell viability. In B16F10 cells, expression levels of cleaved-caspase-3 and Bax were significantly upregulated, while the levels of Bcl-2 and Bcl-xl were downregulated (Fig. 2C). In A375 cells, expression levels of cleaved-caspase-3 and NF-κB p65 were significantly upregulated, while the levels of Bcl-xl were downregulated (Fig. 2D). These results showed that EZP induced melanoma apoptosis by inhibiting anti-apoptotic proteins and activating pro-apoptotic proteins. The above data suggested that EZP restrained melanoma growth associated with induced cell death.

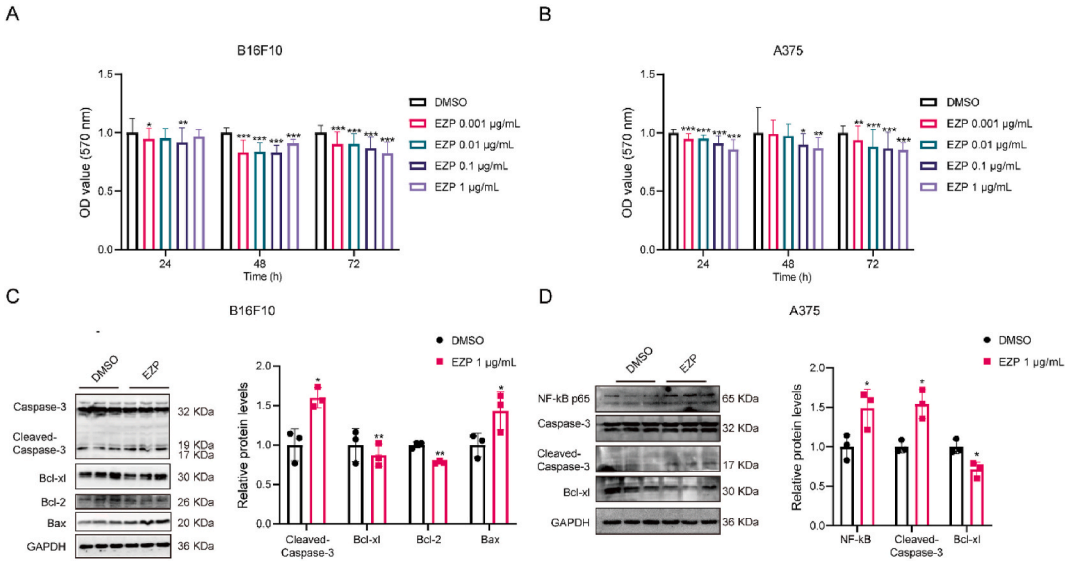

Fig. 2. *In vitro* antitumor activity of EZP extract against melanoma cells. (A and B) Cell proliferation ability of B16F10 (A) and A375 (B) was detected using MTT assay at 24, 48, and 72 h after treatment with different concentrations of EZP (0.001, 0.01, 0.1, 1 μg/mL) for 24, 48, and 72 h n = 7–12. (C and D) Caspase-3, cleaved-caspase-3, Bcl-2, Bax, Bcl-xl and NK-κB p65 protein expression levels with GAPDH serving as a loading control (cleaved-caspase-3 expression levels versus caspase-3) were analyzed by western blotting and quantified after B16F10 (C) and A375 (D) cells treating with 1 μg/mL EZP extract for 48 h n = 3. Data are expressed as mean ± SD. $^{*}P < 0.05$, $^{**}P < 0.01$ and $^{***}P < 0.001$ vs DMSO. DMSO, dimethylsulfoxide; Bcl-2, B-cell lymphoma-2; Bax, Bcl-2 associated X protein; Bcl-xl, Bcl-2 like 1; NF-κB, nuclear factor kappa-B; GAPDH, glyceraldehyde 3-phosphate dehydrogenase.

3.2. A network pharmacology approach to predict potential mechanisms of EZP

To predict potential mechanisms of EZP for melanoma via immune response, network pharmacology was applied as an invaluable tool to describe and analyze its medicinal properties of complex natural products [13,14]. Through searching the PubChem, SwissADME, TCMSP and SwissTargetPrediction databases to obtain active compounds and prediction targets of EZP, combining the compounds information of each database and eliminating the repeated targets, a total of 435 active targets of EZP were obtained. Next, we searched CTD and GeneCards database and screened the known target genes related to melanoma and immune response (Fig. 3A). The intersection of 435 predicted EZP targets, 20765 melanoma targets and 15607 targets of immune response was obtained in Venn diagram to obtain 406 common targets (Fig. 3B). These 406 common targets were considered as potential targets of EZP for the treatment of melanoma via immune response.

Following this lead, a PPI network was constructed using the STRING database and then processed with Cytoscape 3.7.2 software (Fig. 3C). According to the results of PPI network analyses using CytoHubba to calculate degree value, Jun Proto-Oncogene, AP-1 transcription factor subunit (JUN), STAT1, STAT3, NF-κB, RELA, hypoxia inducible factor 1 subunit alpha (HIF-1α), AKT serine/threonine kinase 1 (AKT1) and phosphoinositide-3-kinase regulatory subunit 1 (PI3KR1) were the key nodes (Fig. 3D). The GO analysis revealed that EZP affects a list of genes associated with cell proliferation, cell cycle, cell apoptosis and T cell activation, and the KEGG pathways analysis stated that JAK-STAT signaling pathway and T cell receptor signaling pathway might be involved during EZP treatment (Fig. 3E and F). STAT1, and STAT3 have been recognized as the key regulatory proteins within the JAK-STAT signaling axis. Additionally, JUN, NF-κB, RELA, AKT1, and PI3KR1 have been identified as the principal regulatory proteins involved in the T cell receptor signaling axis. Interestingly, it has become abundantly clear that these proteins play critical roles in activating T cell pathway [15]. More experimental evidence is required to evaluate the potential immunopharmacological effects of EZP.

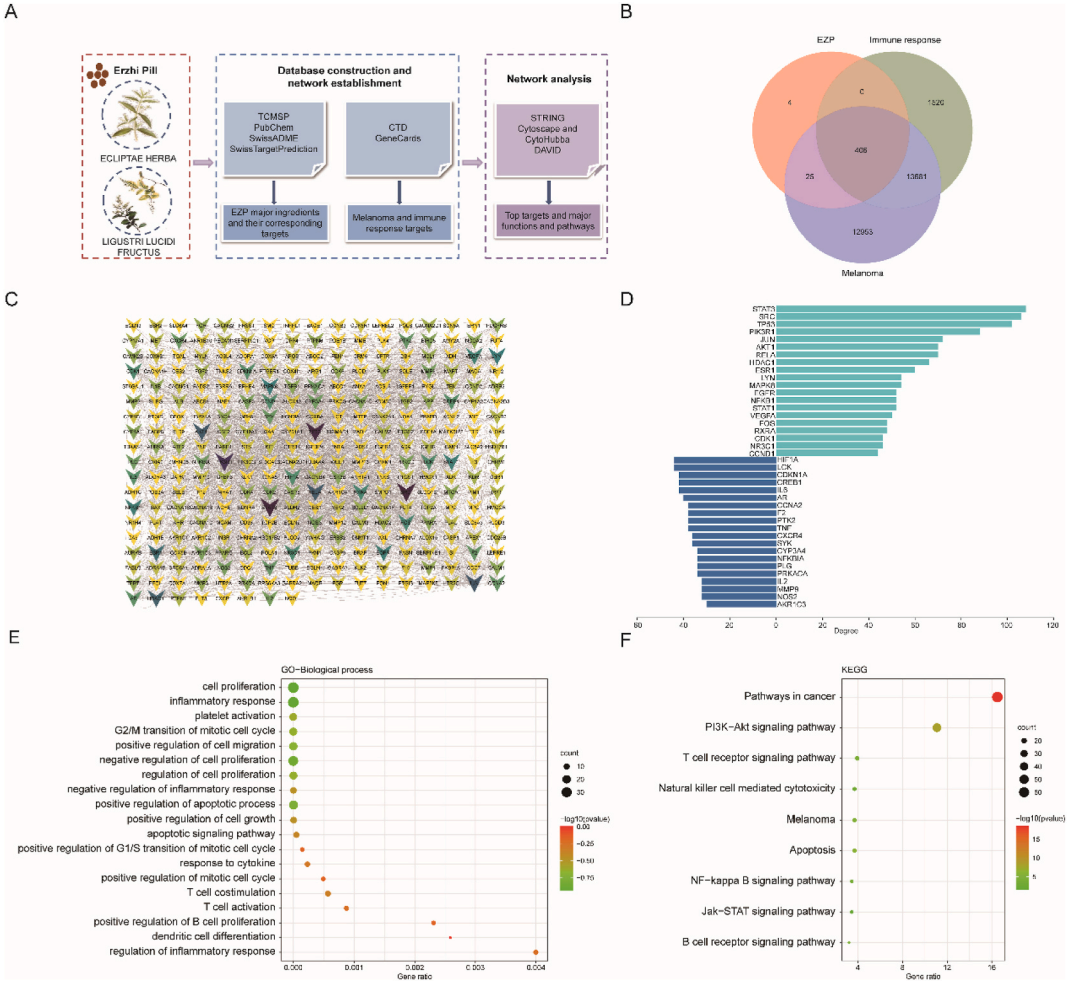

Fig. 3. Network pharmacology of EZP for melanoma via immune response. (A) The overall workflow of network pharmacological study of EZP. (B) VENN diagram of the number of target genes of EZP, melanoma and immune response and their common targets. (C and D) PPI analysis. (C) PPI network of common target. (D) Barplot graph of the key common targets of degree in the PPI network. (E) GO functional enrichment analysis. (F) KEGG pathway enrichment analysis. PPI, protein-protein interaction; GO, gene ontology; KEGG, kyoto encyclopedia of genes and genomes.

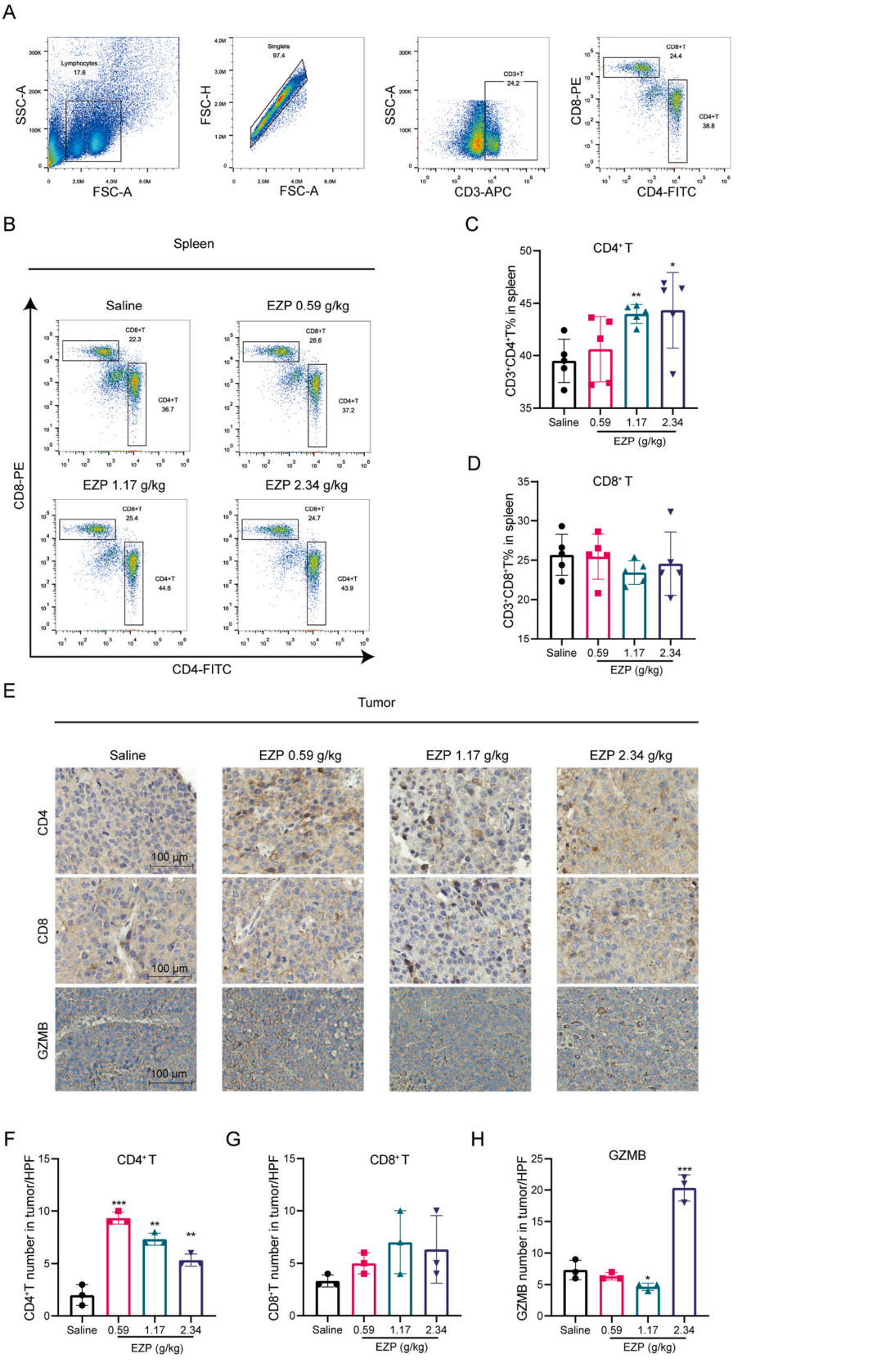

(caption on next page)

Fig. 4. EZP increased the percentage of $CD4^+$ T cells and enhanced the function of $CD8^+$ T *in vivo*. (A–D) T cells were analyzed by flow cytometry. (A) The gate strategy for $CD4^+$ and $CD8^+$ T cells. Flow cytometry plots (B) and bar graphs present percentages of $CD3^+CD4^+$ T cells (C) and $CD3^+CD8^+$ T cells (D) in the spleen from each group mice. n = 5. (E–H) IHC staining for the tumor tissues. IHC images (E) and quantifications of $CD4^+$ T cells (F), $CD8^+$ T cells (G) and $GZMB^+$ cells (H) in tumor tissues. Scale bar, 100 μm. n = 3. Data are expressed as mean ± SD. $^*P < 0.05$, $^{**}P < 0.01$ and $^{***}P < 0.001$ vs DMSO. IHC, immunohistochemistry; GZMB, granzyme B.

3.3. EZP increased the number of $CD4^+$ T cells and enhanced the function of $CD8^+$ T cells in vivo

T cell responses could dictate tumor regression or progress. $CD8^+$ T cells have the ability to selectively detect and eradicate cancer cells by producing IFN-γ, GZMB and perforin. $CD4^+$ T cells help increase the cell-intrinsic anti-tumor activity of $CD8^+$ T cell by multiple complementary mechanisms [16–18]. Most cancer immunotherapies require T cells to perform anti-neoplastic effects. Fig. 4A presents a flow cytometry gating strategy for $CD4^+$ and $CD8^+$ T cells. We observed the role of T cells in the inhibitory effects of EZP in melanoma growth. The administration of EZP significantly increased percentages of $CD3^+CD4^+$ T cells in spleen and the infiltration of $CD4^+$ T cells in tumor tissue (Fig. 4B, C, 4E and 4F). However, EZP did not significantly affect the proportions of $CD8^+$ T cells in spleen and tumor (Fig. 4E and G). We examined $CD8^+$ T cell function by evaluating intracellular expression of granzyme B. As illustrated in Fig. 4E and H, EZP at clinically equivalent dose (2.34 g/kg) could elevate the expression of granzyme B, indicating EZP may exert its anti-tumor effect by enhancing function of $CD8^+$ T cells.

3.4. EZP enhanced the cytotoxic activity of T cells

To determine the extent of fratricide among T cells against melanoma cells, the killing assay was further performed in order to study T cell cytotoxicity using a co-culture model. Jurkat cell line is a human T-leukemic cell line suitable to mimic cultured T cells. The flow

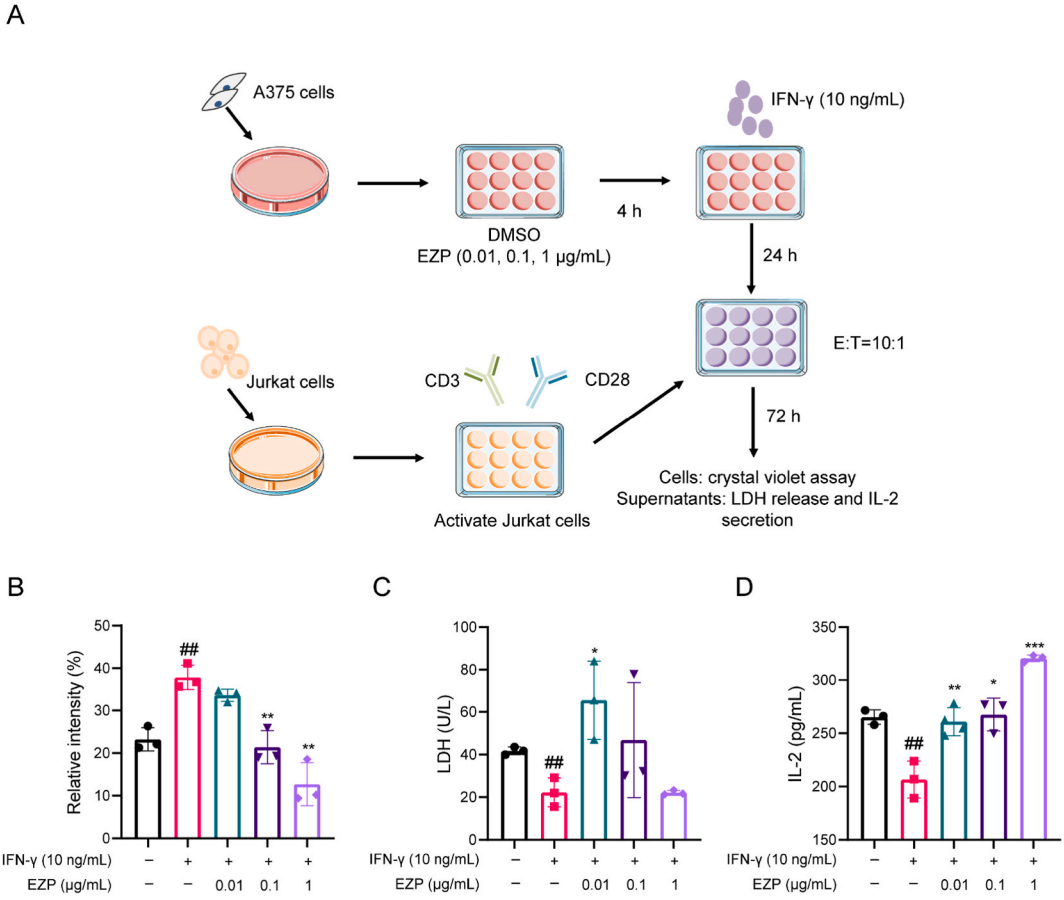

Fig. 5. EZP enhanced the killing ability of T cells on melanoma cells. (A) Schematic of experimental design for co-culture experiments of Jurkat and A375 cells. Co-cultures at an effector-to-target (E:T) ratio of 10:1 were incubated for 72 h. (B) Crystal violet staining assay. (C) LDH release was measured by an LDH assay. (D) The secretion of IL-2 was measured in co-culture supernatants. n = 3–4. Data are expressed as mean ± SD. $^{\#\#}P < 0.01$ vs DMSO. $^*P < 0.05$, $^{**}P < 0.01$ and $^{***}P < 0.001$ vs IFN-γ group. LDH, lactate dehydrogenase assay; IFN-γ, interferon-γ. (For interpretation of the references to colour in this figure legend, the reader is referred to the Web version of this article.)

chart of the experimental design is shown in Fig. 5A. After co-culture for 72 h, CV staining showed a greater number of surviving cells in the IFN-γ treatment alone group than EZP treatment group (Fig. 5B). Moreover, compared with the IFN-γ treatment group, EZP increased LDH release in the culture supernatant (Fig. 5C). IL-2 mainly produced by $CD4^+$ T cells and promoted $CD8^+$ T cells cytotoxicity activity is used to treat metastatic melanoma [19]. In co-culture experiment, IFN-γ decreased the production of IL-2, while increased IL-2 secretion was observed after EZP treatment (Fig. 5D). These results indicated that EZP could enhance the cytotoxic activity of T cells *in vitro*.

3.5. EZP decreased the expression of PD-L1 in vitro and in vivo

In tumor microenvironment, IFN-γ secreting by infiltrating immune cells activated STAT signaling and promoted PD-L1 expression in tumor cells [20,21]. The JAK/STAT signaling pathway is involved in the control of PD-L1 gene expression via different downstream transcription factors, such as STAT1 and NF-κB [22–25]. PD-L1 is widely found in cancer cells including melanoma cells [24,26,27]. Activating PD-L1 pathway could reduce anti-tumor activity of T cells and induce T-cell apoptosis, eventually leading to tumor immune escape [22]. Antibodies or drugs targeting PD-L1 activate anti-tumor immune reaction [25]. We investigated whether IFN-γ induced PD-L1 expression and compared the mechanisms by which EZP influenced IFN-γ-induced PD-L1 expression in A375 cells. To induce expression of PD-L1, A375 cells were treated with 10 ng/mL IFN-γ for 24 h in culture media. Afterwards, A375 cells were administrated with EZP extract at different concentrations for 48 h. As shown in Fig. 6A–D, the expression of NF-κB, p-STAT1 and PD-L1 was increased after IFN-γ stimulation but there was no significant difference ($P > 0.05$). After EZP treatment, NF-κB and p-STAT1 decreased although the difference did not reach significance ($P > 0.05$, Fig. 6A–C). PD-L1 was significantly reduced in EZP-treated groups (Fig. 6A–D). In animal models the same trend was mirrored (Fig. 6E and F). Taken together, we speculated that a reduction of PD-L1 expression directly or indirectly upon EZP treatment may depend on the inhibition of the STAT signaling pathway or NF-κB signaling pathway.

4. Discussion

In this work, we demonstrated that EZP could exert its anti-tumor effect associated with enhanced functions of T cells via inhibiting the expression of PD-L1 (Fig. 7).

Cancer immunotherapy, which aims at activating human immune system to recognize and eliminate cancer cells, is emerging as a next-generation cancer treatment [28]. Different forms of cancer immunotherapy, including oncolytic virus therapies (e.g. Imlygic), cancer vaccines (e.g. sipulucel-T and GVAX), cytokine therapies (e.g. IL-2 and IFN-α), adoptive cell transfer (e.g. chimeric antigen receptor (CAR) T cells and CAR-natural killer (NK) cells) and immune checkpoint inhibitors (e.g. CTLA-4, PD-1/PD-L1), have been proven effective in several tumors [29,30]. Despite many strengths, cancer immunotherapy still has some limitations including contributing to adverse effect profile and toxicity, drug resistance or even relapse and fully effective for a few patients [31,32]. While cancer immunotherapies can be used to treat at any time during the disease progression, there is still a need for immune agents that can be used either alone or in concert with surgery, chemotherapy, radiotherapy, and other cancer therapies.

TCM and related nutritional support therapy have been found to be promising methods of treating cancer. Given the pharmacological effects of tonics, immune regulation and anti-tumor activity of EZP which has few deleterious side effects [12,33–36], our

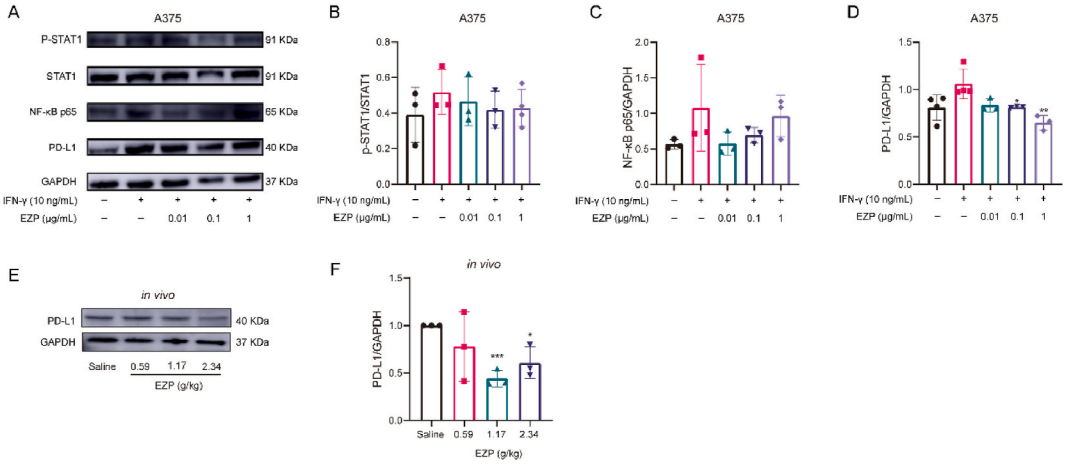

Fig. 6. A reduction of PD-L1 expression upon EZP treatment. (A–D) p-STAT1, NK-κB p65 and PD-L1 protein expression levels were analyzed by western blotting after treating A375 cells with EZP extract for 48 h (A). The protein levels of p-STAT1 (B), NK-κB p65 (C) and PD-L1(D) were respectively quantified. n = 3–4. Data are expressed as mean ± SD. $^*P < 0.05$, $^{**}P < 0.01$ and $^{***}P < 0.001$ vs IFN-γ group. (E–F) PD-L1 protein expression levels were analyzed by western blotting *in vivo*. n = 3. Data are expressed as mean ± SD. $^*P < 0.05$, $^{**}P < 0.01$ and $^{***}P < 0.001$ vs IFN-γ group or saline. p-STAT1, phospho-signal transducer and activator of transcription 1. PD-L1, programmed cell death-ligand 1.

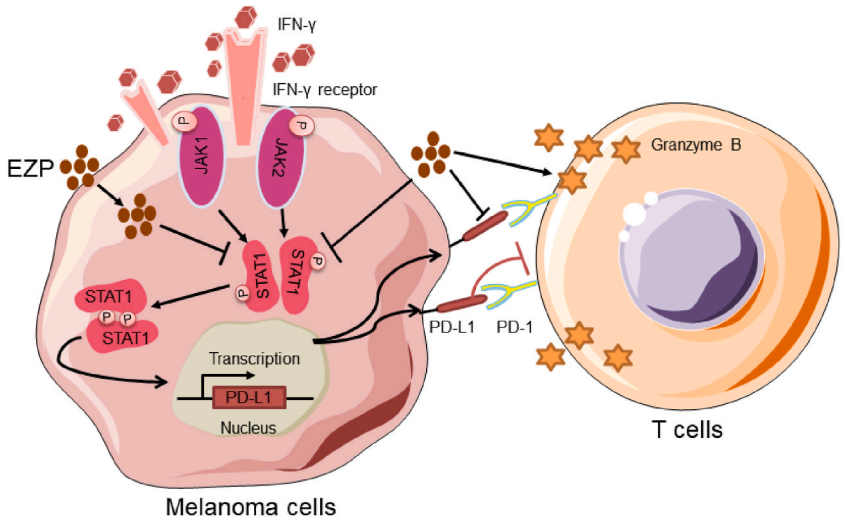

Fig. 7. EZP could exert its antitumor effect through immunoregulation. EZP treatment directly or indirectly reduced the expression of PD-L1.

results represented that EZP exerted anti-tumor effects through immune regulation. Our preliminary experimental results showed that EZP had a poor anti-tumor effect when administered to mice after tumor formation (data not shown). We administered the drug on the day the mice were inoculated with tumor cells [37,38]. The results showed that EZP effectively limited the growth rate of tumors in mice administered on the day of modeling. The results suggested that, as an immunomodulatory Chinese medicine, EZP could suppress tumor growth by activating immune system and play a crucial role in preventing tumorigenesis. Given that EZP has shown similar effects across various stages of the disease, it may offer potential benefits as an adjuvant therapy for cancer.

EZP increased the numbers of $CD4^+$ T cells in spleen and melanoma tissues. $CD4^+$ T cells were demonstrated to assist $CD8^+$ T response including secreting GZMB [16]. In tumor immunity, $CD4^+$ T cells can activate $CD8^+$ T cells through various mechanisms, causing them to differentiate into cytotoxic T lymphocytes (CTLs), while maintaining and enhancing the anti-tumor response of CTLs. In addition, even without $CD8^+$ T cells, $CD4^+$ T cells can secrete IFN-γ to directly kill tumor cells. Our finding highlighted the critical role of $CD4^+$ T cells after EZP treatment during cancer therapies.

It was found that 2.34 g/kg EZP (clinically equivalent dose) significantly increased the expression of GZMB in tumor tissues, suggesting $CD8^+$ T cell function was enhanced in EZP-treated group. GZMB was produced by $CD8^+$ T cells and NK cells, which are major players of antitumor immunity [18,39,40].

In the tumor microenvironment, PD-L1 is highly expressed in tumor cells and tumor-related antigen-presenting cells. Under long-term stimulation of tumor antigens, PD-1 is highly expressed in tumor infiltrating lymphocytes. The combination of PD-L1 and PD-1 can induce T cell apoptosis, inactivation and depletion, thus inhibiting the activation, proliferation and anti-tumor function of tumor antigen-specific $CD8^+$ T cells, and realizing tumor immune escape [25]. Recently, there has been a degree of success in clinical trials utilizing antibodies to inhibit immune checkpoints for the purpose of antitumor therapy. Nevertheless, immune checkpoint inhibitors can lead to adverse effects, such as the onset of significant inflammation, which could pose a life-threatening risk if not effectively controlled. An upregulated immune response may lead to additional side effects. Hence, additional research is necessary to determine the suitable method for administering anti-PD-L1 agents in a clinical context. Our data showed that EZP reduced the expression of PD-L1, indicating that a joint treatment combining EZP and PD-L1 blockade may represent a promising strategy for treating human cancers. The JAK/STAT signaling pathway is involved in the control of PD-L1 gene expression via different downstream transcription factors, such as STAT1 and NF-κB [20,22,25,38]. IFN-γ is a PD-L1 inducer [41], and our results revealed a similar trend although the difference did not achieve significance. A reduction of PD-L1 expression directly or indirectly upon EZP treatment could depend on the inhibition of the JAK-STAT signaling pathway.

EZP at high dose (2.34 g/kg) was calculated according to the conversion table of equivalent effective dose ratios from human to animals based on the body surface area. The medium and low doses were obtained by diluting twice and four times the high dose, respectively. Among them, 0.59 g/kg EZP has the best effect, indicating that it is more effective. We speculated EZP may play a different biological role in different cells or different physiological and pathological conditions. In the future, we will continue to explore the characteristics of different doses of EZP to clarify its pharmacological effects.

To sum up, EZP could not only indirectly kill melanoma cells by influencing tumor immune microenvironment, enhancing the functions of T cells, but also had a certain inhibitory effect on melanoma cells themselves, reflecting the advantages of TCM in curing diseases via multiple targets, multiple pathways, and multiple links (Fig. 7). The impact of EZP on the immune system is multifaceted and intricate, since EZP contains rich and diverse chemical constituents that possess various biological functions that have wide-ranging effects on the immune system, encompassing both innate and adaptive immunity. The facilitation of antitumor immunity by EZP presents a promising approach to cancer treatment. However, there are some limitations of EZP in cancer therapies. First of all, with EZP containing rich and diverse chemical components, it's very difficult to know exactly which ingredient from EZP is responsible

for the net effects. In addition, EZP has an anti-tumor effect on melanoma, and its effect on other types of tumors remains to be determined. Finally, more extensive studies such as integrating multi-omics data and employing computational methods to comprehend tumor biology are warranted to verify the safety and effectiveness of EZP for the treatment of cancer [42,43]. As no study is flawless, these results still gave us a good inspiration that EZP may turn out to be effective treatments in cancers and improve quality of life and survival prospects of patients to supply pharmacological proof supporting its clinical employment.

5. Conclusion

In this work, EZP exerted anti-melanoma effect by blocking PD-1/PD-L1 to activate T cells (Fig. 7). This work presented that EZP might represent a promising candidate drug for cancer immunotherapies and supplied pharmacological proof supporting its clinical employment.

Ethics approval and consent to participate

The protocols for animal expriments were approved by the Ethics Committee of Tianjin University of Traditional Chinese Medicine (approval number TCM-LAEC2021214, registered on February 10, 2021).

Funding statement

This study was supported by The Science & Technology Development Fund of Tianjin Education Commission for Higher Education [Grant number: 2021ZD026], the National Natural Science Foundation of China, China [Grant number: 82174205 and 82274135], and Young Crops Project of Second Affiliated Hospital of Tianjin University of Traditional Chinese Medicine, China [Grant number: QMJH202108].

Data availability statement

Data will be made available on request.

CRediT authorship contribution statement

Zhirui Fang: Writing – review & editing, Writing – original draft, Validation, Methodology, Formal analysis, Data curation. **Yuejin Xue:** Writing – original draft, Methodology, Formal analysis, Data curation. **Yuze Leng:** Validation, Methodology, Formal analysis, Data curation. **Lusha Zhang:** Methodology, Investigation. **Xiuyun Ren:** Software, Methodology, Investigation, Data curation. **Ning Yang:** Software, Methodology, Investigation, Funding acquisition, Data curation. **Jing Chen:** Writing – review & editing, Writing – original draft, Validation, Supervision, Resources, Methodology, Formal analysis. **Lu Chen:** Writing – review & editing, Writing – original draft, Validation, Supervision, Resources, Methodology, Funding acquisition, Formal analysis. **Hong Wang:** Supervision, Resources, Methodology, Funding acquisition.

Declaration of competing interest

The authors declare the following financial interests/personal relationships which may be considered as potential competing interests:Jing Chen, Lu Chen, Hong Wang, Lusha Zhang has patent #ZL 2020 1 1324145.9 licensed to jing Chen, Xiumei Gao, Lu Chen, Hong Wang, Lusha Zhang. If there are other authors, they declare that they have no known competing financial interests or personal relationships that could have appeared to influence the work reported in this paper.

Acknowledgments

There was no special acknowledgment issue.

Appendix A. Supplementary data

Supplementary data to this article can be found online at https://doi.org/10.1016/j.heliyon.2024.e24988.

References

[1] Q. Fu, X. Liu, H. Xia, Y. Li, Z. Yu, B. Liu, X. Xiong, G. Chen, Interferon-γ induces immunosuppression in salivary adenoid cystic carcinoma by regulating programmed death ligand 1 secretion, Int. J. Oral Sci. 14 (2022) 47, https://doi.org/10.1038/s41368-022-00197-x.

[2] Z. Wang, N. Li, K. Feng, M. Chen, Y. Zhang, Y. Liu, Q. Yang, J. Nie, N. Tang, X. Zhang, C. Cheng, L. Shen, J. He, X. Ye, W. Cao, H. Wang, W. Han, Phase I study of CAR-T cells with PD-1 and TCR disruption in mesothelin-positive solid tumors, Cell, Mol. Immunol. 18 (2021) 2188–2198, https://doi.org/10.1038/s41423-021-00749-x.

[3] K. Benesova, F.V. Kraus, R.A. Carvalho, H. Lorenz, C.H. Hörth, J. Günther, K.D. Klika, J. Graf, L. Diekmann, T. Schank, P. Christopoulos, J.C. Hassel, H.-M. Lorenz, M. Souto-Carneiro, Distinct immune-effector and metabolic profile of $CD8^+$ T cells in patients with autoimmune polyarthritis induced by therapy with immune checkpoint inhibitors, Ann, Rheum. Dis. 81 (2022) 1730–1741, https://doi.org/10.1136/ard-2022-222451.

[4] G. Shamai, A. Livne, A. Polónia, E. Sabo, A. Cretu, G. Bar-Sela, R. Kimmel, Deep learning-based image analysis predicts PD-L1 status from H&E-stained histopathology images in breast cancer, Nat. Commun. 13 (2022) 6753, https://doi.org/10.1038/s41467-022-34275-9.

[5] E. Dodagatta-Marri, D.S. Meyer, M.Q. Reeves, R. Paniagua, M.D. To, M. Binnewies, M.L. Broz, H. Mori, D. Wu, M. Adoumie, R. Del Rosario, O. Li, T. Buchmann, B. Liang, J. Malato, F. Arce Vargus, D. Sheppard, B.C. Hann, A. Mirza, S.A. Quezada, M.D. Rosenblum, M.F. Krummel, A. Balmain, R.J. Akhurst, α-PD-1 therapy elevates Treg/Th balance and increases tumor cell pSmad3 that are both targeted by α-TGFβ antibody to promote durable rejection and immunity in squamous cell carcinomas, J. Immunother. Cancer. 7 (2019) 62, https://doi.org/10.1186/s40425-018-0493-9.

[6] A.M. Nash, M.I. Jarvis, S. Aghlara-Fotovat, S. Mukherjee, A. Hernandez, A.D. Hecht, P.D. Rios, S. Ghani, I. Joshi, D. Isa, Y. Cui, S. Nouraein, J.Z. Lee, C. Xu, D. Y. Zhang, R.A. Sheth, W. Peng, J. Oberholzer, O.A. Igoshin, A.A. Jazaeri, O. Veiseh, Clinically translatable cytokine delivery platform for eradication of intraperitoneal tumors, Sci. Adv. 8 (2022), https://doi.org/10.1126/sciadv.abm1032 eabm1032.

[7] T. Tong, H. Hu, J. Zhou, S. Deng, X. Zhang, W. Tang, L. Fang, S. Xiao, J. Liang, Glycyrrhizic-acid-based Carbon Dots with high antiviral activity by multisite inhibition mechanisms, Small 16 (2020) 1906206, https://doi.org/10.1002/smll.201906206.

[8] J. Meng, X. Ai, Y. Lei, W. Zhong, B. Qian, K. Qiao, X. Wang, B. Zhou, H. Wang, L. Huai, X. Zhang, J. Han, Y. Xue, Y. Liang, H. Zhou, S. Chen, T. Sun, C. Yang, USP5 promotes epithelial-mesenchymal transition by stabilizing SLUG in hepatocellular carcinoma, Theranostics 9 (2019) 573–587, https://doi.org/10.7150/thno.27654.

[9] F. Ren, Y. Zhang, Y. Qin, J. Shang, Y. Wang, P. Wei, J. Guo, H. Jia, T. Zhao, Taraxasterol prompted the anti-tumor effect in mice burden hepatocellular carcinoma by regulating T lymphocytes, Cell Death Dis. 8 (2022) 264, https://doi.org/10.1038/s41420-022-01059-5.

[10] X. Li, X. Lu, D. Fan, L. Li, C. Lu, Y. Tan, Y. Xia, H. Zhao, M. Fan, C. Xiao, Synergistic effects of erzhi pill combined with methotrexate on osteoblasts mediated via the wnt1/LRP5/β-catenin signaling pathway in collagen-induced arthritis rats, Front. Pharmacol. 11 (2020) 228, https://doi.org/10.3389/fphar.2020.00228.

[11] X. Zhao, X. Zhao, Z. Huang, M. Zhou, Study on the effects of the active site of the pill on SOD, MDA, MAO, LPF and aging-related proteins P16 and P21 in rats with D-galactose aging model, J. Tradit. Chin. Med. (2023) 35–40.

[12] H. Yang, J. Mao, Clinical study of Erzhi Wan and Guizhi decoction in the treatment of triple-negative breast cancer[J], Chinese J. Moder. App. Phar. 39 (05) (2022) 658–662, https://doi.org/10.13748/j.cnki.issn1007-7693.2022.05.014.

[13] C. Huang, C. Zheng, Y. Li, Y. Wang, A. Lu, L. Yang, Systems pharmacology in drug discovery and therapeutic insight for herbal medicines, Brief, Bioinform 15 (2014) 710–733, https://doi.org/10.1093/bib/bbt035.

[14] S. Zhao, S. Li, Network-based relating pharmacological and genomic spaces for drug target identification, PLoS One 5 (2010) e11764, https://doi.org/10.1371/journal.pone.0011764.

[15] C. Sun, R. Mezzadra, T.N. Schumacher, Regulation and function of the PD-L1 checkpoint, Immunity 48 (2018) 434–452, https://doi.org/10.1016/j.immuni.2018.03.014.

[16] J. Borst, T. Ahrends, N. Bąbała, C.J.M. Melief, W. Kastenmüller, $CD4^+$ T cell help in cancer immunology and immunotherapy, Nat. Rev. Immunol. 18 (2018) 635–647, https://doi.org/10.1038/s41577-018-0044-0.

[17] D. Ostroumov, N. Fekete-Drimusz, M. Saborowski, F. Kühnel, N. Woller, CD4 and CD8 T lymphocyte interplay in controlling tumor growth, Cell. Mol. Life Sci. 75 (2018) 689–713, https://doi.org/10.1007/s00018-017-2686-7.

[18] M. Philip, A. Schietinger, CD8+ T cell differentiation and dysfunction in cancer, Nat. Rev. Immunol. 22 (2022) 209–223, https://doi.org/10.1038/s41577-021-00574-3.

[19] T. Jiang, C. Zhou, S. Ren, Role of IL-2 in cancer immunotherapy, OncoImmunology 5 (2016) e1163462, https://doi.org/10.1080/2162402X.2016.1163462.

[20] J.E. Darnell, L.M. Kerr, G.R. Stark, Jak-STAT pathways and transcriptional activation in response to IFNs and other extracellular signaling proteins, Science 264 (1994) 1415–1421, https://doi.org/10.1126/science.8197455.

[21] M. Hira-Miyazawa, H. Nakamura, M. Hirai, Y. Kobayashi, H. Kitahara, G. Bou-Gharios, S. Kawashiri, Regulation of programmed-death ligand in the human head and neck squamous cell carcinoma microenvironment is mediated through matrix metalloproteinase-mediated proteolytic cleavage, Int. J. Oncol. (2017), https://doi.org/10.3892/ijo.2017.4221.

[22] H. Dong, S.E. Strome, D.R. Salomao, H. Tamura, F. Hirano, D.B. Flies, P.C. Roche, J. Lu, G. Zhu, K. Tamada, V.A. Lennon, E. Celis, L. Chen, Tumor-associated B7-H1 promotes T-cell apoptosis: a potential mechanism of immune evasion, Nat. Med. 8 (2002) 793–800, https://doi.org/10.1038/nm730.

[23] D. Schadendorf, A.C.J. Van Akkooi, C. Berking, K.G. Griewank, R. Gutzmer, A. Hauschild, A. Stang, A. Roesch, S. Ugurel, Melanoma, The Lancet 392 (2018) 971–984, https://doi.org/10.1016/S0140-6736(18)31559-9.

[24] H. Yamaguchi, J.-M. Hsu, W.-H. Yang, M.-C. Hung, Mechanisms regulating PD-L1 expression in cancers and associated opportunities for novel small-molecule therapeutics, Nat. Rev. Clin. Oncol. 19 (2022) 287–305, https://doi.org/10.1038/s41571-022-00601-9.

[25] W. Zou, J.D. Wolchok, L. Chen, PD-L1 (B7-H1) and PD-1 pathway blockade for cancer therapy: mechanisms, response biomarkers, and combinations, Sci. Transl. Med. 8 (2016), https://doi.org/10.1126/scitranslmed.aad7118.

[26] D.B. Johnson, J.A. Sosman, Therapeutic advances and treatment options in metastatic melanoma, JAMA Oncol. 1 (2015) 380, https://doi.org/10.1001/jamaoncol.2015.0565.

[27] E. Jaune, E. Cavazza, C. Ronco, O. Grytsai, P. Abbe, N. Tekaya, M. Zerhouni, G. Beranger, L. Kaminski, F. Bost, M. Gesson, M. Tulic, P. Hofman, R. Ballotti, T. Passeron, T. Botton, R. Benhida, S. Rocchi, Discovery of a new molecule inducing melanoma cell death: dual AMPK/MELK targeting for novel melanoma therapies, Cell Death Dis. 12 (2021) 64, https://doi.org/10.1038/s41419-020-03344-6.

[28] Y. Yang, Cancer immunotherapy: harnessing the immune system to battle cancer, J. Clin. Invest. 125 (2015) 3335–3337, https://doi.org/10.1172/JCI83871.

[29] M. Daher, K. Rezvani, Outlook for new CAR-based therapies with a focus on CAR NK cells: what lies beyond CAR-engineered T cells in the race against cancer, Cancer Discov. 11 (2021) 45–58, https://doi.org/10.1158/2159-8290.CD-20-0556.

[30] Y. Zhang, Z. Zhang, The history and advances in cancer immunotherapy: understanding the characteristics of tumor-infiltrating immune cells and their therapeutic implications, Cell, Mol. Immunol. 17 (2020) 807–821, https://doi.org/10.1038/s41423-020-0488-6.

[31] F.B. Bombelli, C.A. Webster, M. Moncrieff, V. Sherwood, The scope of nanoparticle therapies for future metastatic melanoma treatment, Lancet Oncol. 15 (2014) e22–e32, https://doi.org/10.1016/S1470-2045(13)70333-4.

[32] P.S. Hegde, D.S. Chen, Top 10 challenges in cancer immunotherapy, Immunity 52 (2020) 17–35, https://doi.org/10.1016/j.immuni.2019.12.011.

[33] M. Cao, J. Wu, Y. Peng, B. Dong, Y. Jiang, C. Hu, L. Yu, Z. Chen, Ligustri Lucidi Fructus, a traditional Chinese Medicine: comprehensive review of botany, traditional uses, chemical composition, pharmacology, and toxicity, J. Ethnopharmacol. 301 (2023) 115789, https://doi.org/10.1016/j.jep.2022.115789.

[34] B. Chen, L. Wang, L. Li, R. Zhu, H. Liu, C. Liu, R. Ma, Q. Jia, D. Zhao, J. Niu, M. Fu, S. Gao, D. Zhang, Fructus Ligustri lucidi in osteoporosis: a review of its pharmacology, phytochemistry, pharmacokinetics and safety, Molecules 22 (2017) 1469, https://doi.org/10.3390/molecules22091469.

[35] L. Gao, C. Li, Z. Wang, X. Liu, Y. You, H. Wei, T. Guo, Ligustri Lucidi Fructus as a traditional Chinese medicine: a review of its phytochemistry and pharmacology, Nat. Prod. Res. 29 (2015) 493–510, https://doi.org/10.1080/14786419.2014.954114.

[36] J. Zuo, C. Park, M. Doschak, R. Löbenberg, Are the release characteristics of Erzhi pills in line with traditional Chinese medicine theory? A quantitative study, J. Integr. Med. 19 (2021) 50–55, https://doi.org/10.1016/j.joim.2020.10.004.

[37] J. Huang, D. Liu, Y. Wang, L. Liu, J. Li, J. Yuan, Z. Jiang, Z. Jiang, W.W. Hsiao, H. Liu, I. Khan, Y. Xie, J. Wu, Y. Xie, Y. Zhang, Y. Fu, J. Liao, W. Wang, H. Lai, A. Shi, J. Cai, L. Luo, R. Li, X. Yao, X. Fan, Q. Wu, Z. Liu, P. Yan, J. Lu, M. Yang, L. Wang, Y. Cao, H. Wei, E.L.-H. Leung, Ginseng polysaccharides alter the gut microbiota and kynurenine/tryptophan ratio, potentiating the antitumour effect of antiprogrammed cell death 1/programmed cell death ligand 1 (anti-PD-1/PD-L1) immunotherapy, Gut 71 (2022) 734–745, https://doi.org/10.1136/gutjnl-2020-321031.

[38] L. Michel, I. Helfrich, U.B. Hendgen-Cotta, R.-I. Mincu, S. Korste, S.M. Mrotzek, A. Spomer, A. Odersky, C. Rischpler, K. Herrmann, L. Umutlu, C. Coman, R. Ahrends, A. Sickmann, S. Löffek, E. Livingstone, S. Ugurel, L. Zimmer, M. Gunzer, D. Schadendorf, M. Totzeck, T. Rassaf, Targeting early stages of cardiotoxicity from anti-PD1 immune checkpoint inhibitor therapy, Eur. Heart J. 43 (2022) 316–329, https://doi.org/10.1093/eurheartj/ehab430.
[39] J.A. Myers, J.S. Miller, Exploring the NK cell platform for cancer immunotherapy, Nat. Rev. Clin. Oncol. 18 (2021) 85–100, https://doi.org/10.1038/s41571-020-0426-7.
[40] Y. Yamashita, Y. Yatabe, T. Tsuzuki, A. Nakayama, Y. Hasegawa, H. Kojima, T. Nagasawa, N. Mori, Perforin and granzyme expression in cytotoxic T-cell lymphomas, Mod. Pathol. Off. J. U. S. Can. Acad. Pathol. Inc. 11 (1998) 313–323.
[41] X. Zhang, Y. Zeng, Q. Qu, J. Zhu, Z. Liu, W. Ning, H. Zeng, N. Zhang, W. Du, C. Chen, J. Huang, PD-L1 induced by IFN-γ from tumor-associated macrophages via the JAK/STAT3 and PI3K/AKT signaling pathways promoted progression of lung cancer, Int. J. Clin. Oncol. 22 (2017) 1026–1033, https://doi.org/10.1007/s10147-017-1161-7.
[42] F. Ahmed, I.S. Kang, K.H. Kim, A. Asif, C.S.A. Rahim, A. Samantasinghar, F.H. Memon, K.H. Choi, Drug repurposing for viral cancers: a paradigm of machine learning, deep learning, and virtual screening-based approaches, J. Med. Virol. 95 (2023) e28693, https://doi.org/10.1002/jmv.28693.
[43] F. Ahmed, A. Samantasinghar, A.M. Soomro, S. Kim, K.H. Choi, A systematic review of computational approaches to understand cancer biology for informed drug repurposing, J. Biomed. Inform. 142 (2023) 104373, https://doi.org/10.1016/j.jbi.2023.104373.